Supplementary Information

Self Assembly of Ultrathin Au Nanowires into Expanded Hexagonal Superlattice Studied by in situ SAXS

Anaïs Loubat, Marianne Impéror-Clerc, Lise-Marie Lacroix, Brigitte Pansu, Florian Meneau, Bertrand Raquet, and Guillaume Viau.

1. Model for the SAXS intensity.

The SAXS results after background subtraction have been interpreted using a model with three contributions for the intensity (measured in absolute scale, cm^{-1} units): spherical gold nanoparticles, gold nanowires and a hexagonal phase of nanowires, plus a small remaining background constant C :

$$I(q) = I_{sphere}(q) + I_{NW}(q) + I_{Bragg}(q) + C$$

All data have been modeled in a similar way as in references [1-5], in the context of the self-assembly of silica nano-structured materials, using a least-square fitting procedure. Typical values of C less than 0.02 cm^{-1} were used in the fits.

- **Spheres contribution:**

A polydisperse form factor of spheres was used, with no structure factor contribution because of the very low overall volume fraction:

$$I_{sphere}(q) = n_S\left(\rho_{gold} - \rho_0\right)^2 P_{sphere}(q)$$

where n_s is the number density of the spheres and ρ_{gold} and ρ_0 the scattering length densities of gold and hexane. For SAXS, the scattering length density is the product of the classical radius of the electron r_e = 2.81794×10^{-15} m by the electron density (number of electrons per unit volume). The values are known from literature: $\rho_{gold} = r_e\rho^e_{gold}$ and $\rho_0 = r_e\rho^e_0$, with $\rho^e_{gold} = 4650\ e\ nm^{-3}$ and $\rho^e_{hexane} = 230\ e\ nm^{-3}$.

The amplitude form factor of a sphere of radius R *is* $f_S(q,R)$:

$$f_S(q,R) = 3\left(\sin(qR) - qR\cos(qR)\right)/(qR)^3$$

and $V_S = \left(4\pi/3\right)R^3$.

The averaged spherical form factor is:

$$P_{sphere}(q) = < F_S^2(q) > = < V_S^2 f_S^2(q) >$$

where < > stands for the average over the polydispersity (parameter σ) using a Schulz-Zimm distribution:

$$< F_S^2(q,R) > = \int p(r,R,\sigma) F_S^2(q,r) dr$$

$$p(r,R,\sigma) = f_{SZ}(r,R,1/\sigma^2 - 1)$$

$$f_{SZ}(x,x_0,z) = \frac{x^z}{\Gamma(z+1)} \left(\frac{z+1}{x_0} \right)^{z+1} \exp\left(-(z+1)\frac{x}{x_0} \right)$$

The volume fraction ϕ_S of spheres in solution was derived as follows: $n_S = \phi_S / < V_S >$

$$\boxed{I_{Sphere}(q) = (\rho_{gold} - \rho_0)^2 \phi_S \frac{< V_S^2 f_S^2(q,R) >}{< V_S >}}$$

- **Nanowires contribution:**

A form factor for wires of constant length L and average radius R_{NW} was used, with no structure factor contribution:

$$I_{NW}(q) = n_{NW} (\rho_{gold} - \rho_0)^2 P_{NW}(q)$$

where n_{NW} is the number density of the nanowires and ρ_{gold} and ρ_0 the scattering length densities of gold and hexane, like for the spheres.

Polydispersity was introduced only for the radius R_{NW} and the length was fixed to L = 100 nm. Because of the large aspect ratio of the nanowires, the form factor could be factorized in two terms, where < > stands for the average over the polydispersity (parameter σ) using a Schulz-Zimm distribution as for the spheres.

$$P_{NW}(q) = P_{rod}(q) < F_{CS}^2(q) >$$

where $F_{CS}(q)$ is the form factor of the NW's cross-section of radius R_{NW}

$$F_{CS}(q) = \pi R_{NW}^2 \frac{2J_1(qR_{NW})}{qR_{NW}}$$

$$P_{rod}(q) = L^2 \left(\frac{2\sin \mathrm{I}(qL)}{qL} - \frac{4\sin^2(\frac{qL}{2})}{(qL)^2} \right) \text{ with } \quad \sin \mathrm{I}(x) = \int_0^x \frac{\sin u}{u} du$$

For q>>1/L, $P_{rod}(q)$ exhibits the characteristic q^{-1} power low dependence:

$$P_{rod}(q) \cong \frac{\pi L}{q}$$

The volume fraction ϕ_{NW} of nanowires in solution was derived as follows:

$$n_{NW} = \phi_{NW} / < V_{NW} >$$

$$I_{NW}(q) = (\rho_{gold} - \rho_0)^2 \phi_{NW} \frac{P_{rod}(q) < F_{CS}^2(q) >}{L\pi < R_{NW}^2 >}$$

$$\boxed{I_{NW}(q) = (\rho_{gold} - \rho_0)^2 \phi_{NW} \frac{< F_{CS}^2(q) >}{q < R_{NW}^2 >}}$$

- **Hexagonal phase:**

The contribution was modeled by the powder average of a long-range 2D-hexagonal lattice of nanowires:

$$I_{Bragg}(q) = n (\rho_{gold} - \rho_0)^2 \, P_{NW}(q) \left[1 - \beta(q) G(q) + \beta(q) G(q) Z_0(q) \right]$$

$$Z_0(q) = \frac{1}{s_{cell}} \frac{2\pi}{q} \sum_{hk} m_{hk} L_{hk}(q, q_{hk})$$

where s_{cell} is the area of the 2D-hexagonal unit cell and m_{hk} is the multiplicity of each Bragg peak.

The same form factor $P_{NW}(q)$ was used as for the nanowires in solution. The Bragg peaks were recorded at discrete positions q_{hk}. The Bragg peaks were modeled using peak-shaped functions $L_{hk}(q, q_{hk})$ with Gaussian/Lorentzian profiles with a width inversely proportional to the average domain size *D* of the hexagonal domains, corresponding to the diameter of the fiber/bundle around 70 nm. The essential contribution to the Bragg intensities was the form factor $P_{NW}(q)$ of the gold nanowires. But in addition, two types of disorder were included in the model. First a small polydispersity over the nanowires radius (parameter $\sigma = 0.012$), through the average over the cross-section form factor, term $\beta(q)$, . Second, a positional disorder was introduced through the Debye-Waller term $G(q)$:

$$\beta(q) = \frac{< F_{CS}(q) >^2}{< F_{CS}^2(q) >}$$

$$G(q) = \exp(-q^2 \sigma_{DW}^2 a^2)$$

Typical values of σ_{DW} = 0.08 were used for the relative mean-square displacement in the Debye-Waller term.

References:

[1] Sundblom, A.; Oliveira, C. L. P.; Palmqvist, A. E. C.; Pedersen, J. S. *J. Phys. Chem. C* **2009**, *113*, 7706.
[2] Manet, S.; Lecchi, A.; Imperor-Clerc, M.; Zholobenko, V.; Durand, D.; Oliveira, C. L. P.; Pedersen, J. S.; Grillo, I.; Meneau, F.; Rochas, C. *J Phys Chem B* **2011**, *115*, 11318.
[3] Manet, S.; Schmitt, J.; Imperor-Clerc, M.; Zholobenko, V.; Durand, D.; Oliveira, C. L. P.; Pedersen, J. S.; Gervais, C.; Baccile, N.; Babonneau, F.; Grillo, I.; Meneau, F.; Rochas, C. *J Phys Chem B* **2011**, *115*, 11330
[4] Michaux, F., Baccile, N., Impéror-Clerc, M., Malfatti, L., Folliet, N., Gervais, C., Manet, S., Meneau, F., Pedersen, J. S., Babonneau, F. *Langmuir* **2012**, *28*, 17477-17493 .
[5] Schmitt, J.; Impéror-Clerc, M. ; Michaux, F. ; Blin, J. L.; Stébé, M. J.; Pedersen, J.S. ; Meneau, F. *Langmuir* **2013**, *29*, 2007–2023.

3. Supplementary figures

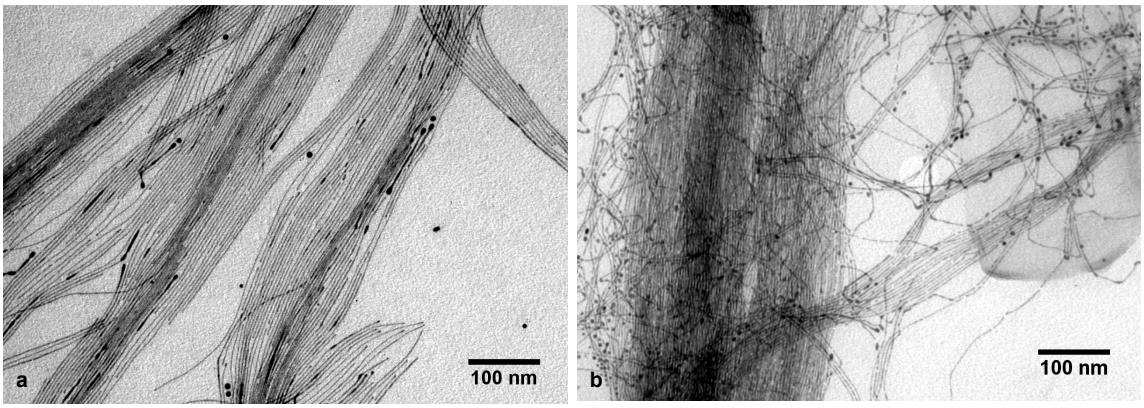

Figure S1: TEM image of Au NPs obtained after 3h at 40°C for TIPS/Au = 100 and [OY] = 400 for a) undisturbed solution or b) under magnetic stirring.

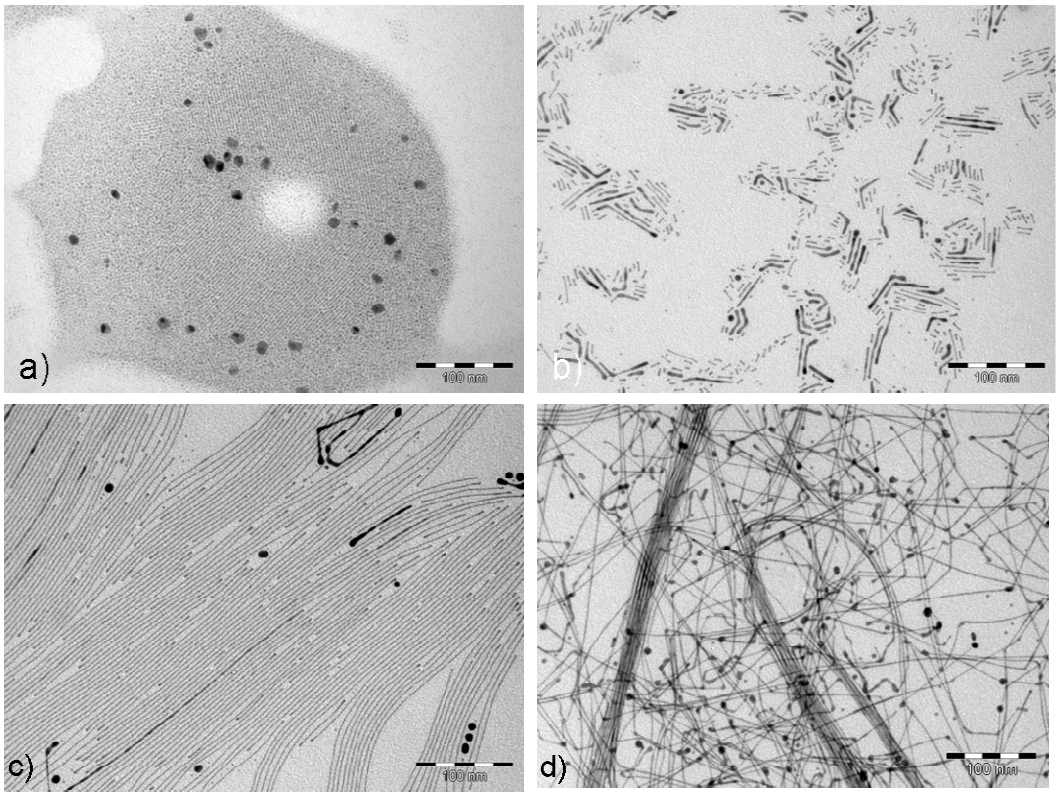

Figure S2: TEM image of Au NPs obtained after 5h at 40°C for TIPS/Au = 100 and [OY] = a) 20 ; b) 50 ; c) 100 and d) 250 mM.

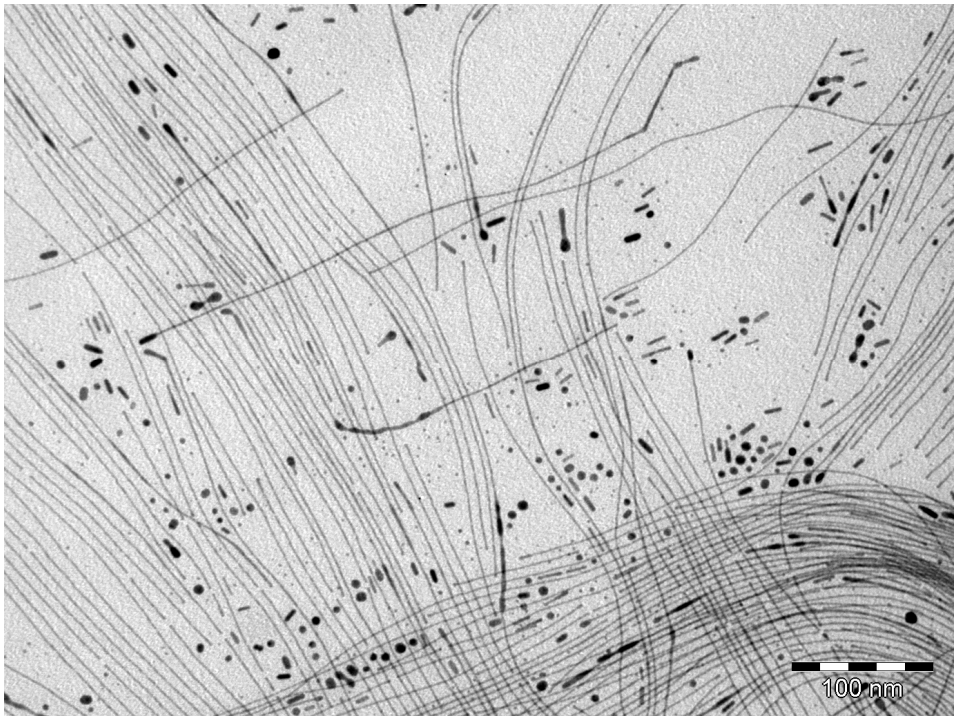

Figure S3: TEM image of Au NPs obtained after 27h at 40°C for TIPS/Au = 100 and [OY] = 400 mM.

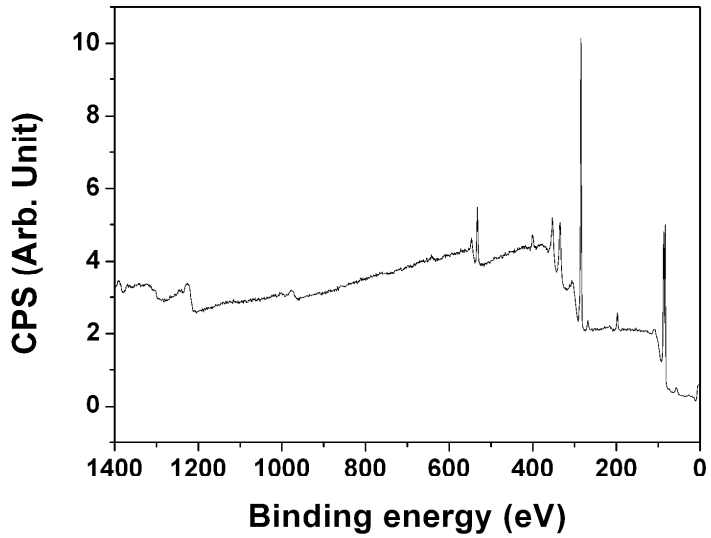

Figure S4: X-ray photon electron survey scan of Au nanowires precipitated by addition of absolute ethanol

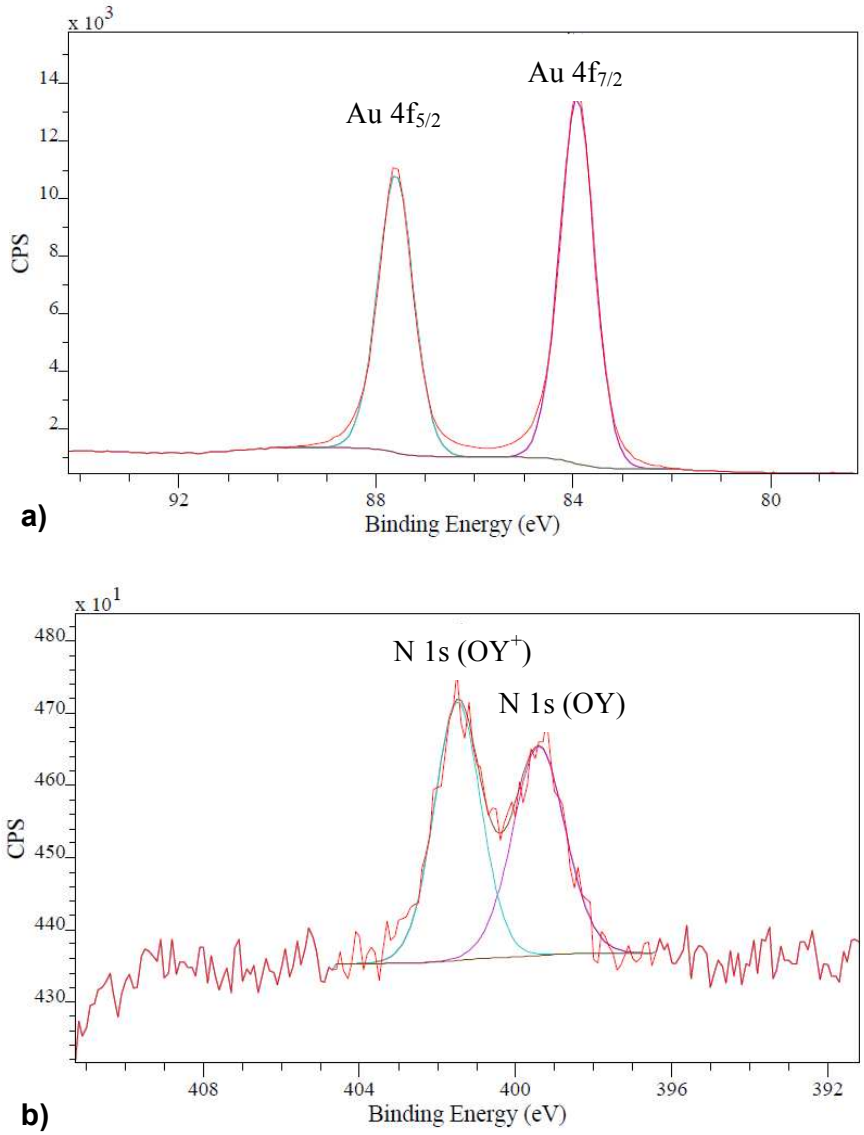

Figure S5: High resolution X-ray photon electron spectra of Au nanowires precipitated by addition of absolute ethanol (a) Au 4f peaks ; (b) N 1s peak and the corresponding fitting profiles

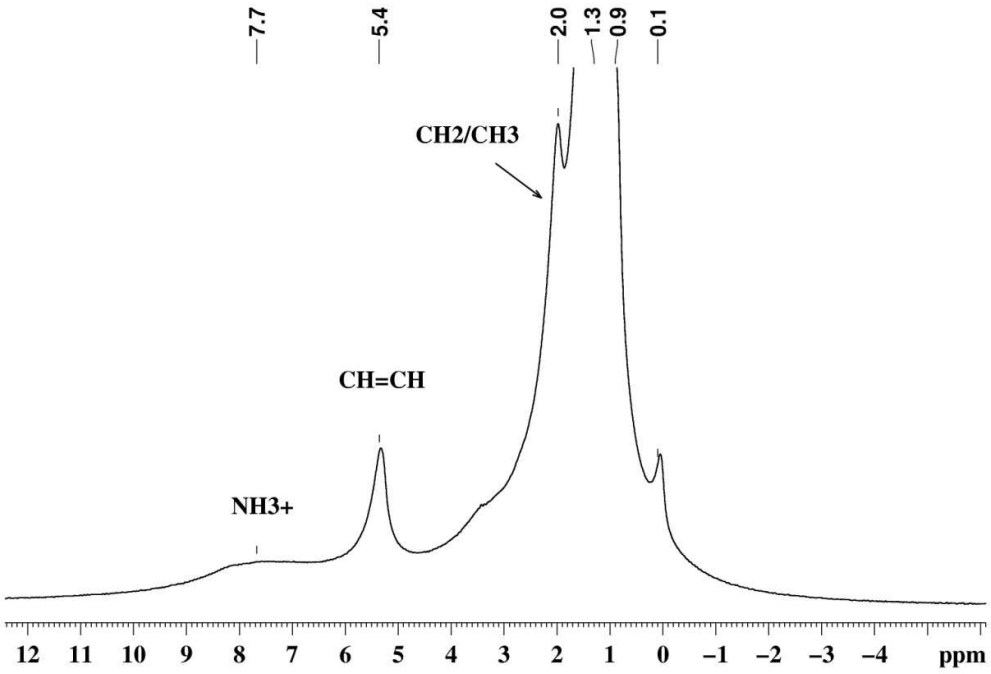

Figure S6: ^{1}H MAS spectrum (spinning rate 24 kHz) of Au NWs after purification.

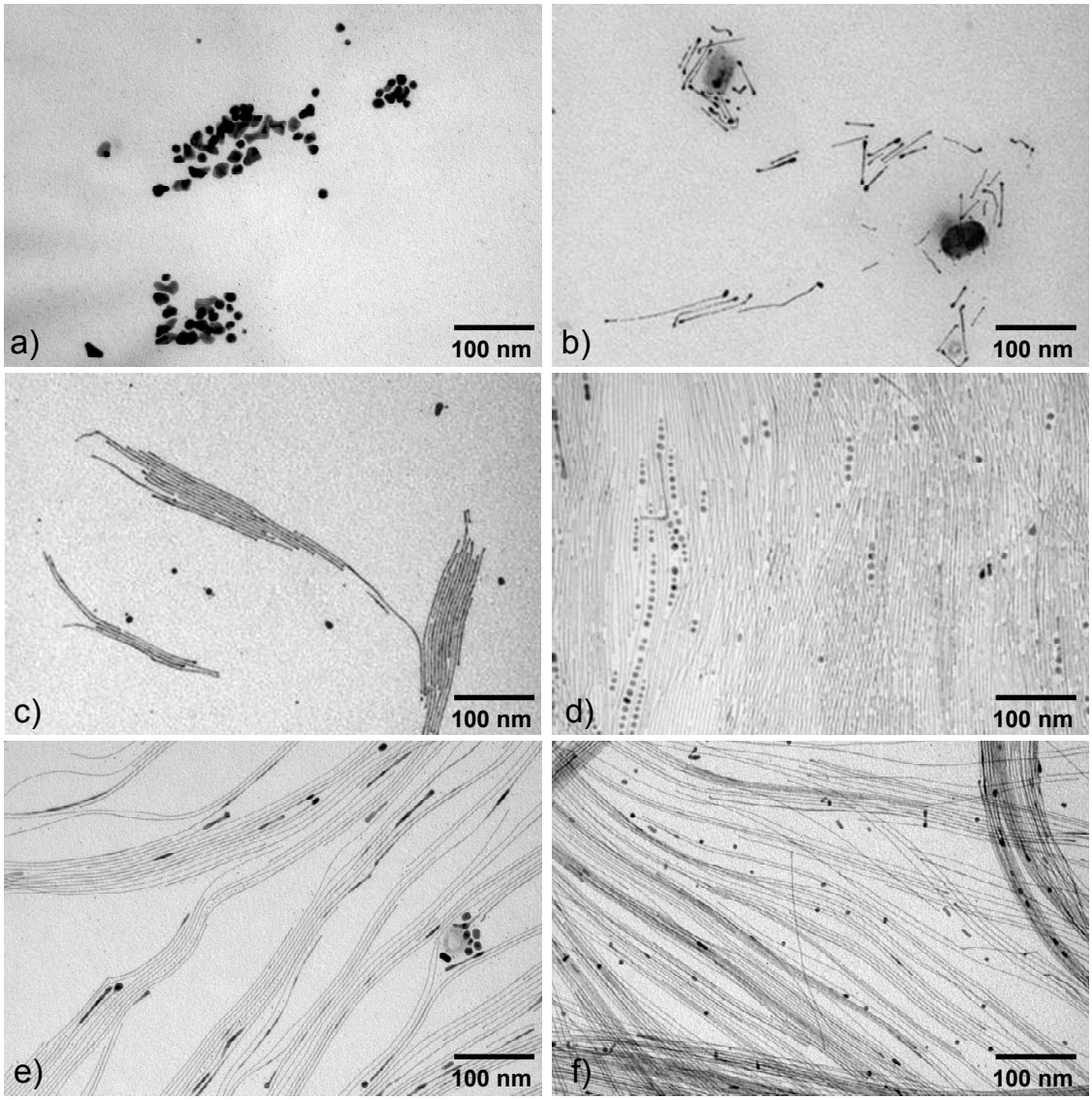

Figure S7. TEM images of Au nanoparticles obtained after a) 1, b) 2, c) 3, d) 4, e) 8 and f) 24 hours of reaction at 25 °C.

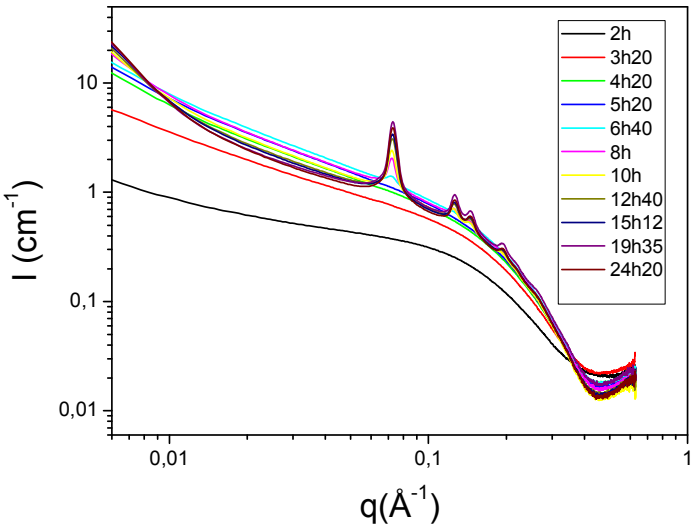

a)

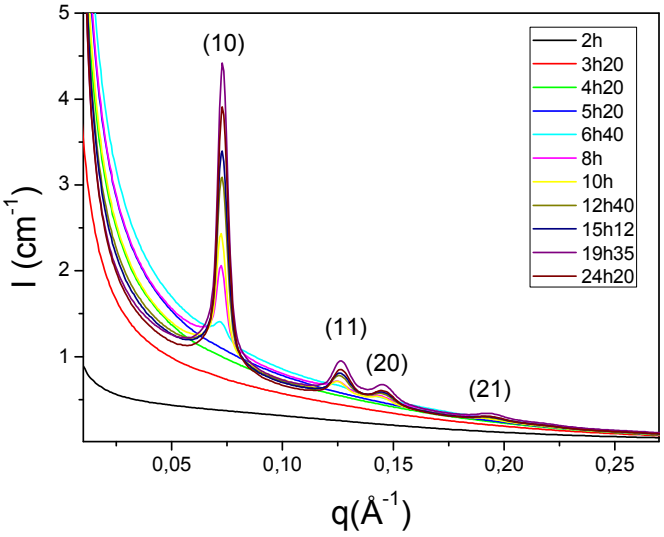

b)

Figure S8: Small angle X-ray scattering results at 25 °C: (a) log-log scale ; (b) linear scale. The hexagonal phase appeared after 6h.

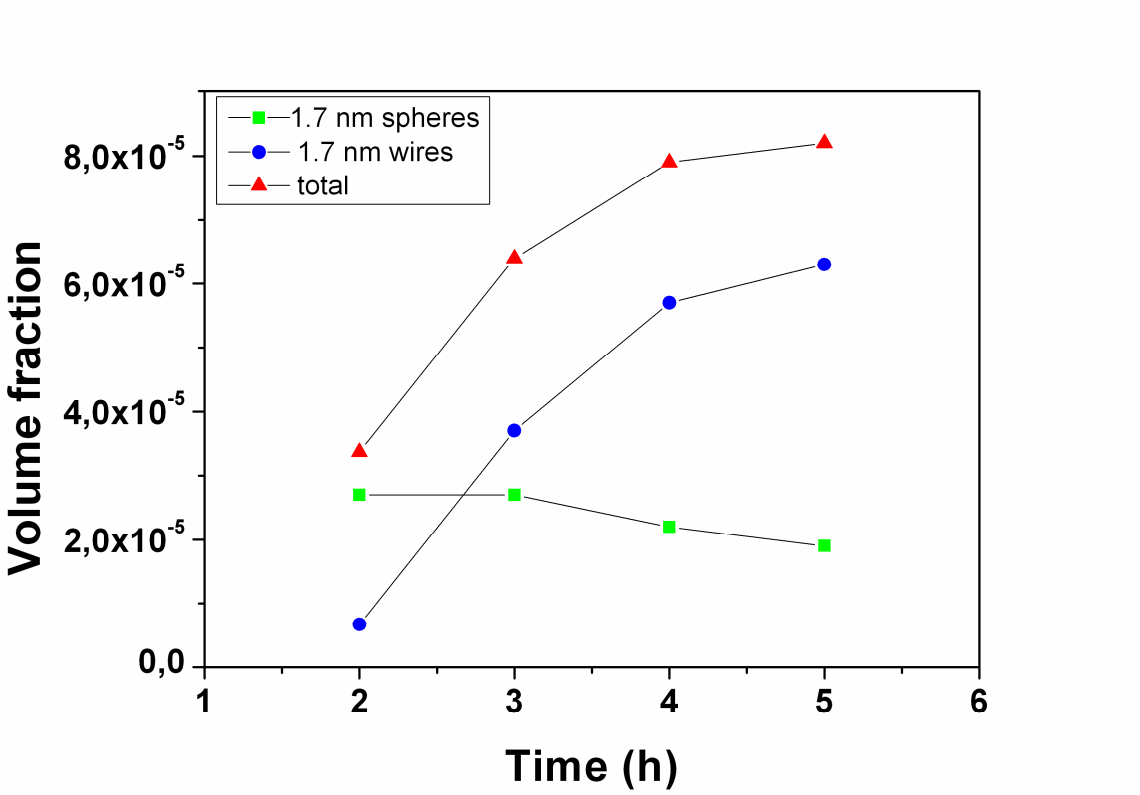

Figure S9: Volume fraction calculated from the SAXS modelling at different time of reaction at 25 °C.

.

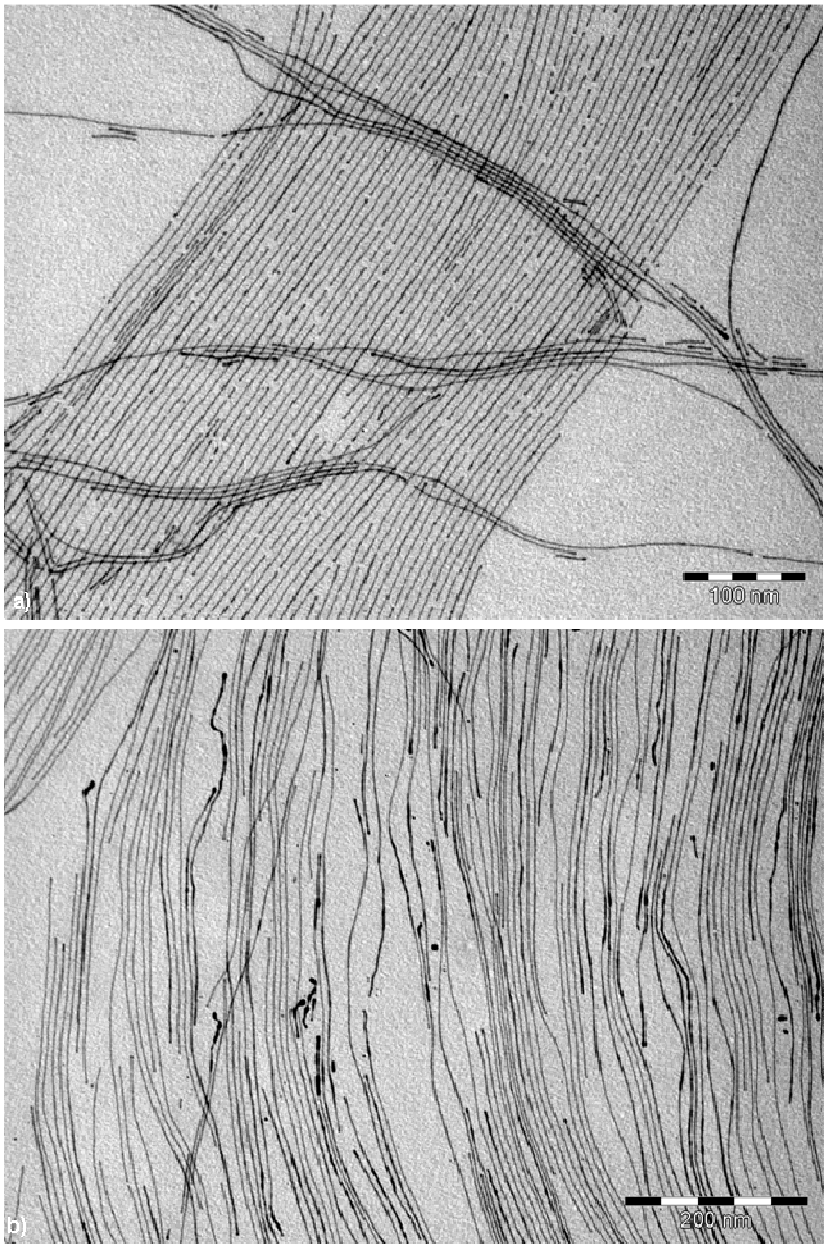

Figure S10. a-b) TEM image of assembled Au NWs.